Calculations of antiproton-nucleus quasi-bound states based on the Paris $\bar{N}N$ potential.

Jaroslava Hrtánková and Jiří Mareš

Nuclear Physics Institute, Řež, Czech Republic

International Conference on Exotic Atoms and Related Topics (EXA2017), 11 - 15 September, 2017, Vienna, Austria

Motivation

- study of $\bar{p}$ interaction with selected nuclei:
  - behavior of $\bar{p}$ in the nuclear medium
  - $\bar{p}$ absorption in a nucleus
  - testing models of (anti)baryon–baryon interactions as well as models for nuclear structure calculations
  - knowledge of $\bar{p}$–nucleus interaction for future experiments (PANDA@FAIR)
- previous study within phenomenological RMF approach
  (J. Hrtánková, J. Mareš, NPA 945 (2016) 197)
  - found $\bar{p}$ widths comparable or larger than binding energies
- Paris $\bar{N}N$ potential recently confronted with $\bar{p}$ atom data
  (E. Friedman, A. Gal, B. Loiseau, S. Wycech, NPA 934 (2015) 101)

Model

- $\bar{p}$ binding energies and widths are obtained by solving the Dirac equation

$$[-i\vec{\alpha}\cdot\vec{\nabla} + \beta m_{\bar{p}} + V_{\rm opt}(r)]\psi_{\bar{p}} = \epsilon_{\bar{p}}\psi_{\bar{p}} \ ,$$

$m_{\bar{p}}$ is the $\bar{p}$ mass, $\epsilon_{\bar{p}} = -B_{\bar{p}} - i\frac{\Gamma_{\bar{p}}}{2}$, $(B > 0)$

- the complex optical potential $V_{\rm opt}(r)$ is of the form

$$2E_{\bar{p}}V_{\rm opt}(r) = q(r) + 3\vec{\nabla}\cdot\alpha(r)\vec{\nabla} \ \ ,$$

with $E_{\bar{p}} = m_{\bar{p}} - B_{\bar{p}}$

- the S-wave part is constructed in a '$t\rho$' form

$$q(r) = -4\pi\left[F_0\frac{1}{2}\rho_p(r) + F_1\left(\frac{1}{2}\rho_p(r) + \rho_n(r)\right)\right] \ ,$$

where F_0 and F_1 – isospin 0 and 1 in-medium amplitudes, $\rho_p(r)$ ($\rho_n(r)$) is the proton (neutron) density distribution calculated in the RMF NL-SH model

Scattering amplitudes

- in-medium amplitudes F_1 and F_0 obtained from free-space S-wave amplitudes using multiple scattering approach (WRW)
  (*T. Wass, M. Rho, W. Weise, NPA 617 (1997) 449*)

$$F_1 = \frac{\frac{\sqrt{s}}{m_N} f^S_{\bar{p}n}(\delta\sqrt{s})}{1 + \frac{1}{4}\xi_k \frac{\sqrt{s}}{m_N} f^S_{\bar{p}n}(\delta\sqrt{s})\rho(r)} \; , F_0 = \frac{\frac{\sqrt{s}}{m_N}[2f^S_{\bar{p}p}(\delta\sqrt{s}) - f^S_{\bar{p}n}(\delta\sqrt{s})]}{1 + \frac{1}{4}\xi_k \frac{\sqrt{s}}{m_N}[2f^S_{\bar{p}p}(\delta\sqrt{s}) - f^S_{\bar{p}n}(\delta\sqrt{s})]\rho(r)} \; ,$$

where $\delta\sqrt{s} = \sqrt{s} - E_{\mathrm{th}}$, $\xi_k = \frac{9\pi}{p_f^2} 4\int_0^\infty \frac{dt}{t} \exp(iqt) j_1^2(t)$ and $q = \frac{1}{p_f}\sqrt{E_{\bar{p}}^2 - m_{\bar{p}}^2}$

- free-space amplitudes $\rightarrow$ 2009 version of the Paris $\bar{N}N$ potential constrained by $\bar{p}$ scattering and antiproton atom data
  (*B. El-Bennich, M. Lacombe, B. Loiseau, S. Wycech, PRC 79 (2009) 054001*)

In-medium Paris S-wave amplitudes

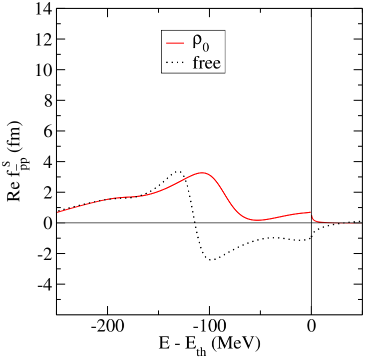

Fig.1: Energy dependence of the Paris 09 $\bar{p}p$ c.m. S-wave amplitudes: Pauli blocked amplitude for $\rho_0 = 0.17$ fm^{-3} (solid lines) compared with free-space amplitude (dotted lines).

In-medium Paris S-wave amplitudes

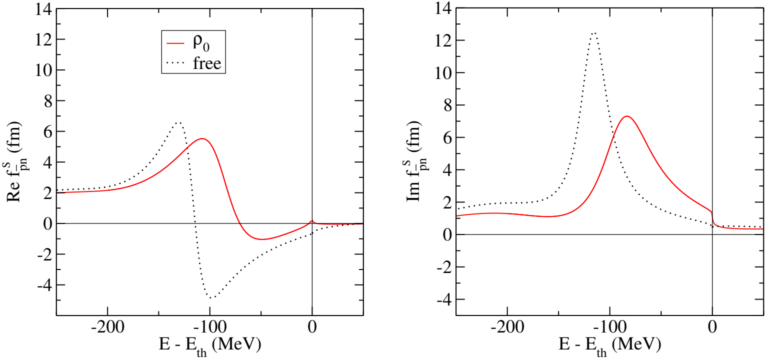

Fig.2: Energy dependence of the Paris 09 $\bar{p}n$ c.m. S-wave amplitudes: Pauli blocked amplitude for $\rho_0 = 0.17$ fm^{-3} (solid lines) compared with free-space amplitude (dotted lines).

Paris P-wave interaction

- The P-wave potential

$$2E_{\bar{p}}V_{\mathrm{opt}}(r) = q(r) + 3\vec{\nabla}\cdot\alpha(r)\vec{\nabla}\ ,$$

where

$$\alpha(r) = 4\pi\frac{m_N}{\sqrt{s}}\left(f^P_{p\bar{p}}(\delta\sqrt{s})\rho_p(r) + f^P_{n\bar{p}}(\delta\sqrt{s})\rho_n(r)\right)\ .$$

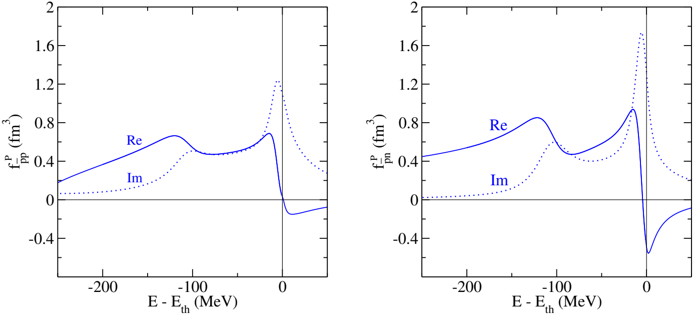

Fig.3: Energy dependence of the Paris 09 $\bar{p}p$ (left) and $\bar{p}n$ (right) c.m. free-space P-wave amplitudes.

P-wave interaction

- S + P-wave Paris potential does not fit the $\bar{p}$ atom data
- S-wave Paris potential + phenomenological P-wave $f^P_{\bar{p}N} = 2.9 + i1.8$ fm^3 yields satisfactory agreement with the atom data
  (E. Friedman, A. Gal, B. Loiseau, S. Wycech, NPA 934 (2015) 101)

Energy dependence

- $\bar{p}N$ Paris amplitudes — functions of energy shift $\delta\sqrt{s} = \sqrt{s} - E_{th}$ where $s = (E_N + E_{\bar{p}})^2 - (\vec{p}_N + \vec{p}_{\bar{p}})^2$

- $\bar{p}$ absorption in a nucleus $\rightarrow$ $\vec{p}_N + \vec{p}_{\bar{p}} \neq 0$
  (*A. Cieplý, E. Friedman, A. Gal, D. Gazda, J. Mareš, PLB 702, 402 (2011)*)

$$\sqrt{s} = E_{th}\left(1 - \frac{2(B_{\bar{p}} + B_{Nav})}{E_{th}} + \frac{(B_{\bar{p}} + B_{Nav})^2}{E_{th}^2} - \frac{1}{E_{th}} T_{\bar{p}} - \frac{1}{E_{th}} T_{Nav}\right)^{1/2},$$

where $B_{Nav} = 8.5$ MeV, $\hat{T} = -\frac{\hbar^2}{2m_N}\triangle$ and $E_{th} = m_N + m_{\bar{p}}$

- self-consistent scheme adopted in the calculations

Energy dependence of the S-wave $\bar{p}$ potential

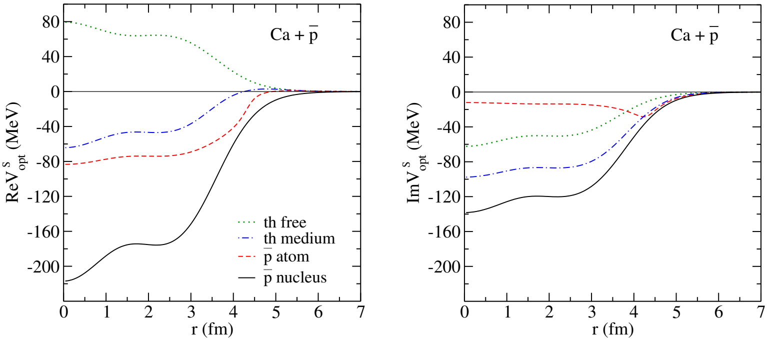

Fig.4: The potential felt by $\bar{p}$ at threshold ('th medium'), in the $\bar{p}$ atom and $\bar{p}$ nucleus, calculated for ^{40}Ca+$\bar{p}$ with in-medium Paris S-wave amplitudes and static RMF densities. The $\bar{p}$ potential calculated using free-space amplitudes at threshold is shown for comparison ('th free').

1s $\bar{p}$ binding energies and widths

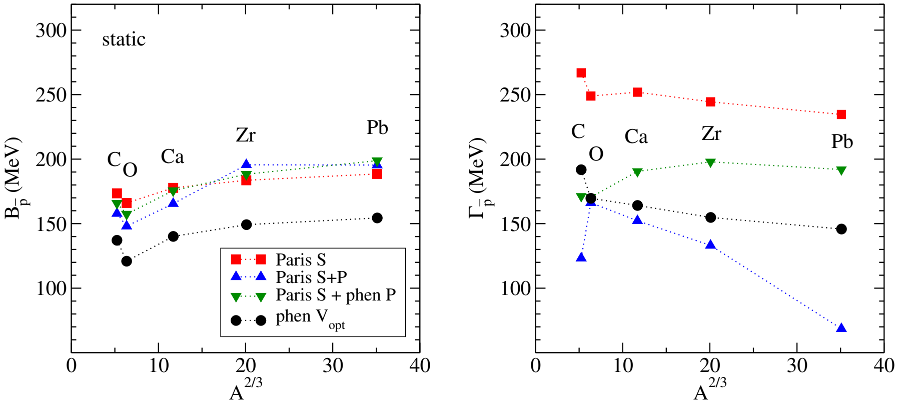

Fig.4: 1s $\bar{p}$ binding energies (left panel) and widths (right panel) in various nuclei, calculated statically using *S*-wave Paris potential, including phenomenological *P*-wave potential, Paris *P*-wave potential and phenomenological RMF potential.

1s $\bar{p}$ binding energies and widths

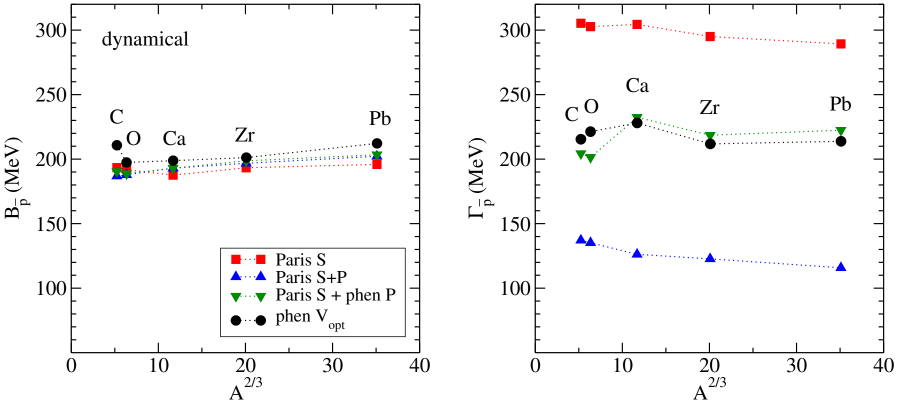

Fig.5: Binding energies (left panel) and widths (right panel) of 1s $\bar{p}$-nuclear states in selected nuclei, calculated dynamically using the Paris $\bar{N}N$ S-wave potential, Paris S-wave + phen. P-wave and phenomenological RMF potential.

$\bar{p}$ binding energies and widths – excited states

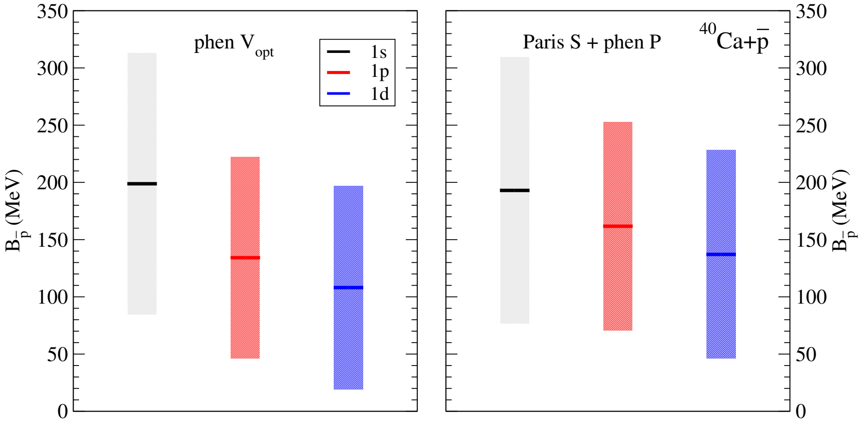

Fig.6:1s, 1p and 1d binding energies (lines) and widths (boxes) of $\bar{p}$ in ^{40}Ca calculated dynamically within the phenomenological RMF $\bar{p}$ optical potential and Paris S-wave + phen. P-wave potential.

Conclusions

- calculations of $\bar{p}$ quasi-bound states in various nuclei with 2009 version of the Paris $\bar{N}N$ potential
- the $\bar{p}$ potential is strongly energy dependent
- P-wave interaction slightly affects the $\bar{p}$ binding energies and decrease noticeably the $\bar{p}$ widths
- Paris $S + P$-wave potential yields too small $\bar{p}$ widths (also fails to reproduce $\bar{p}$ atom data)
- Paris S-wave + phenomenological P-wave potential yield comparable $\bar{p}$ binding energies (~ 200 MeV) and widths ($\sim 200 - 230$ MeV) as the phenomenological approach within the RMF model.

Back up slides

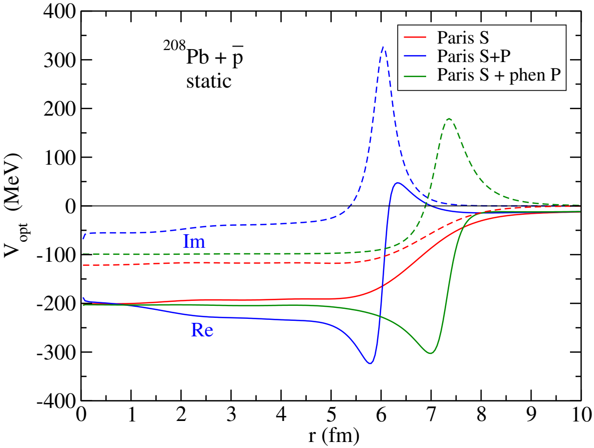

Fig.6:The real (solid curves) and imaginary (dashed curves) parts of the S-wave Paris potential (red) and the local (Krell-Ericson) forms of the Paris $S+P$-wave (green) and Paris S-wave + phen. P-wave (blue) potentials felt by $\bar{p}$ in ^{208}Pb, calculated statically.

Table : Self-consistent energy shifts $\delta\sqrt{s}$ in ^{208}Pb+$\bar{p}$ relevant to static calculations within the Paris S-wave, Paris $S+P$-wave and Paris S-wave + phen. P-wave potentials.

^{208}Pb+$\bar{p}$	Paris S	Paris $S+P$	Paris S + phen. P
$\delta\sqrt{s}$ (MeV)	-210.6	-238.9	-223.6